J. Mt. Sci. (2013) 10(3):355–362
DOI: 10.1007/s11629-013-2564-1

Determining Topographic Shielding from Digital Elevation Models for Cosmogenic Nuclide Analysis: a GIS Approach and Field Validation

LI Ying-kui*

Department of Geography, University of Tennessee, Knoxville, TN 37966, USA

**Corresponding author, e-mail: yli32@utk.edu*

Abstract: Topographic shielding of cosmic radiation flux is a key parameter in using cosmogenic nuclides to determine surface exposure ages or erosion rates. Traditionally, this parameter is measured in the field and uncertainty and/or inconsistency may exist among different investigators. This paper provides an ArcGIS python code to determine topographic shielding factors using digital elevation models (DEMs). This code can be imported into ArcGIS as a geoprocessing tool with a user-friendly graphical interface. The DEM-derived parameters using this method were validated with field measurements in central Tian Shan. Results indicate that DEM-derived shielding factors are consistent with field-measured values. It provides a valuable tool to save fieldwork efforts and has the potential to provide consistent results for different regions in the world to facilitate the comparison of cosmogenic nuclide results.

Keywords: Cosmogenic nuclides; Topographic shielding; ArcGIS; Python; Digital elevation models (DEMs)

Introduction

Cosmogenic nuclides (e.g., ^{10}Be, ^{26}Al, and ^{36}Cl) have been widely used in Earth sciences to determine surface exposure ages, local and spatially integrated erosion rates, and have led to revolutionary developments in the study of geomorphology, quaternary geology, and geochronology (Gosse and Phillips 2001; Bierman and Nichols 2004; Li and Harbor 2009; Balco 2011). Cosmogenic nuclides are produced by the interaction of cosmic ray and minerals at or near the Earth's surface. They are particularly suitable to study Earth surface processes and landform evolution because cosmogenic nuclides are produced just within a few meters of rock and sediment's surfaces (Gosse and Phillips 2001; Li and Harbor 2009).

The production rate of a specific cosmogenic nuclide (such as ^{10}Be) is determined mainly by the geomagnetic latitude and altitude of the sample site (Lal 1991; Dunai 2000; Stone 2000; Desilets and Zreda 2003; Lifton et al. 2005; Desilets et al. 2006; Balco et al. 2008). It is also affected by topography because the topography around a sample site may block a portion of incoming cosmic radiations or modify the effective attenuation length for a slope surface (Dunne et al. 1999; Gosse and Phillips 2001; Codilean 2006). The common way to determine the topographic shielding is to measure the slope and aspect (or strike and dip) of the sample site and record a set of azimuth and elevation angles of topographic obstructions around the sample site in the field (http://hess.ess.washington.edu/math/general/skyline_input.php). It is time-consuming to collect these measurements for a large number of sample sites. It may also lead to uncertainties and/or inconsistency among different investigators due to the potential differences in field-interpreted topographic obstructions and measured azimuth and elevation angle pairs. After collecting these

Received: 16 October 2012
Accepted: 5 March 2013

measurements, topographic shielding at each site can be calculated using computational tools such as the CRONUS-Earth web calculator (Balco et al. 2008) or the Excel-based CosmoCalc calculator (Vermeesch 2007). However, these calculations are impractical for basin-wide erosion studies in mountainous terrains that have gained considerable popularity in recent years (e.g. Wittmann et al. 2007).

The availability of digital elevation models (DEMs) and the development of geographic information systems (GIS) provide the potential to derive the topographic shielding from DEMs using GIS analysis. Codilean (2006) demonstrated a method to derive topographic shielding for large areas using DEMs and shaded relief modeling (hillshade) in GIS. It provided an alternative way to determine the topographic shielding for any given site on the Earth surface. However, there is still not a straightforward tool to implement this analysis and the DEM-derived shielding factors were not validated by field measurements. The purpose of this paper is to provide an easy-to-use ArcGIS python code to derive topographic shielding factors and to validate the DEM-derived values using field measurements in central Tian Shan, western China.

1 Topographic Shielding Factor and the GIS Approach to Derive It

The ideal sites for cosmogenic nuclide analysis are horizontal surfaces at the highest points of the landscape. However, most samples are collected from sites in the vicinity of slopes or topographic obstructions that block part of the cosmic radiation flux due to the realities of the field settings and the particular research questions being addressed (Gosse and Phillips 2001; Li and Harbor 2009). Therefore, the shielding effects of the topographic obstructions for a sample site should be considered (Dunne et al. 1999; Gosse and Phillips 2001). To account for the blocked radiation by topography obstructions, a topographic shielding factor (C_T) can be defined as the ratio of the remaining cosmogenic flux to the maximum flux received by a site with an unshielded exposure (Dunne et al. 1999; Gosse and Phillips 2001; Codilean 2006). Assuming n topographic obstructions can be measured around a sample site and each obstruction has its own azimuth (ϕ_i) and elevation (θ_i) angles, C_T can be calculated by (Dunne et al. 1999; Codilean 2006):

$$C_T = 1 - \frac{1}{2\pi}\sum_{i=1}^{n}\Delta\phi_i \sin^{m+1}(\theta_i) \qquad (1)$$

where m is an experimental constant and equal to 2.3 in most studies (Nishiizumi et al. 1989; Gosse and Phillips 2001; Balco et al. 2008). This equation is only valid for horizontal surfaces with surrounding topographic obstructions (azimuth and elevation angle pairs) from mountains peaks, ridges, slopes, and local minor topographic features (such as boulders). When the shielding from local minor topographic features can be ignored, a set of average azimuth and elevation angles within a small azimuthal bin ($\Delta\phi$) around a site can also be determined from DEMs and the topographic shielding factor, C_T, for the site can be calculated using DEM-derived azimuth and elevation parameters.

The procedure to derive the topographic shielding factor using DEMs is usually computational intensive especially for a large number of sample sites or an entire drainage area. Codilean (2006) proposed to use a common shaded relief modeling function (hillshade) in GIS (Burrough and McDonell 1998) to determine the topographic shielding factor for an area. Instead of determining the azimuth and elevation angles for each individual site, Codilean (2006) used the hillshade function to identify all the DEM cells that are in shadow (blocked by surrounding topography features) and assign them with a value of $\sin^{m+1}(\theta_s)$ for a given illumination azimuth (ϕ_s) and elevation angle (θ_s) and then repeat this operation for a range of illumination azimuth and elevation angle pairs to calculate the shielding factor for the whole area. However, a customized and automated tool to implement this analysis is still lacking. This paper introduced a revised algorithm and a python tool in ArcGIS to implement this analysis.

2 Python Code Design and Implementation in ArcGIS

ArcGIS is a commonly used GIS package and has been widely used in DEM-related spatial analysis. The recent versions of ArcGIS (after version 9.1) provide a Modelbuilder environment and a python script interface to customize and automate GIS spatial analyses. Because the calculation of the topographic shielding factor requires repeating the hillshade function for a range of azimuth and elevation angle pairs, a python code is developed to implement the algorithm proposed by Codilean (2006) and allow for the iteration operation. The following steps were designed based on Equation (1) (Figure 1A):

(a) For each azimuth value, run a set of hillshade functions by continuously increasing elevation angles from 0 to 90 degree using a user defined increment interval (such as 2°) to identify the maximum elevation angles for all DEM cells that can create shadows (in ArcGIS, the shadow cells are assigned with a value of zero). This process will be stopped if no shadows are created for all DEM cells when the elevation angle increases to a certain value. This step will create a raster with the maximum shielding elevation angles for all DEM cells (the cell that will never be shadow has a raster value of zero).

(b) Assign a weight value of $\sin^{m+1}(\theta)$ to each cell based on their corresponding maximum shielding elevation angle (θ) to create a shielding raster for this azimuth value.

(c) Iterate the upper two steps to other azimuth values from 0 to 360 degree using a user defined increment interval to create the shielding raster for each azimuth value.

(d) Average shielding rasters of all azimuth values to calculate the overall shielding raster.

(e) Subtract the overall shielding raster from 1 to get the topographic shielding factor for each DEM cell.

This code requires several input parameters: DEM, the interval values for azimuth and elevation angles (az_interval and el_interval in Figure 1A), and a z_factor parameter representing the ratio between the vertical and horizontal units of the DEM. The output of this code is the topographic shielding factor raster for each DEM cell (Figure 1B).

In ArcGIS, this python code can be imported as a GIS geoprocessing tool into the ArcToolBox with a user friendly graphical user interface (GUI) similar to other standard GIS geoprocessing tools. Figure 1B illustrated the GUI in ArcGIS 10 to perform this python code. Basically, the user just needs to choose the DEM used to calculate the topographic shielding factor, assign the interval values for both azimuth and elevation angles, and provide a file name to save the calculated topographic shielding factor raster. ArcGIS also provides a geoprocessing tool called “Extract Values to Points” to extract raster values to all points in a point shapefile. Therefore, if the sample

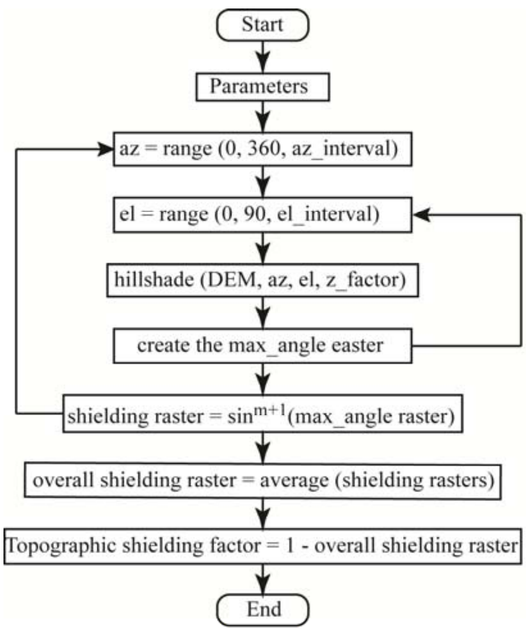

(A)

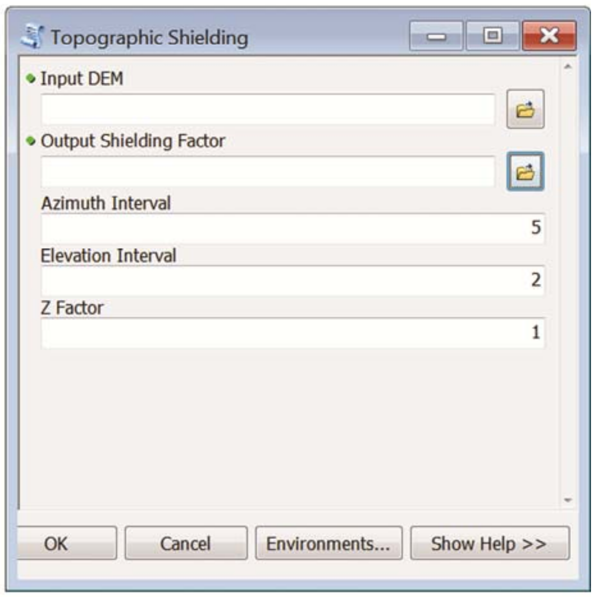

(B)

Figure 1 (A) A flowchart of the python code to calculate topographic shielding factor using DEM. (B) The graphic user interface (GUI) of the python code after importing it as a tool in ArcGIS (version 10) sites are already in a shapefile format, it is straightforward to obtain the DEM-derived topographic shielding factor for each site. If the sample sites are recorded as a text or excel file, it can be converted into a shapefile in ArcGIS. To directly access all these tools, an ArcGIS toolbox can be created to include the python code for the topographic shielding factor calculation and the geoprocessing tools to extract raster values to points and to convert text/excel file to a shapefile for the sample sites. The user can easily add this tool into the ArcToolBox to use these functions (The python code and the ArcGIS toolbox are available at http://web.utk.edu/~yli32/shielding.zip).

3 Validation of DEM-derived Shielding Factors from Central Tian Shan

Field measurements of the topographic shielding factors from central Tian Shan, western China, are used to validate the DEM-derived topographic shielding factors. The central Tian Shan, around the source area of the Urumqi River (Figure 2A), is one of the most intensively studied areas of glacial geomorphology because of its spectacular landforms and the presence of a major research station in the valley since 1959 (e.g., Li et al. 2001, 2011; Zhao et al. 2006; Kong et al. 2009). The fieldwork was conducted in the summer of 2010. A GPS handheld unit was used to record the location of each measured site (latitude, longitude, and altitude). A laser rangefinder with integrated compass and inclinometer, TruPulse 360, was used to measure the azimuth and elevation angle pairs of topographic obstructions around each measured site. This equipment has a compass accuracy (for azimuth angle) of ±1.0° and inclination accuracy (for elevation angle) of ±0.25°. In total, the topographic shielding parameters from ten sites were measured and the measured azimuth and elevation angle pairs are listed in Table 1. The field-measured topographic shielding factor for each site was calculated based on Equation (1) (Table 1).

The DEM-derived topographic shielding factor was calculated using the 3 arc-second (90-m) resolution Shuttle Radar Topography Mission (SRTM) DEM (http://srtm.csi.cgiar.org). The field-measured topographic shielding factors are compared with DEM-derived values using a 5°

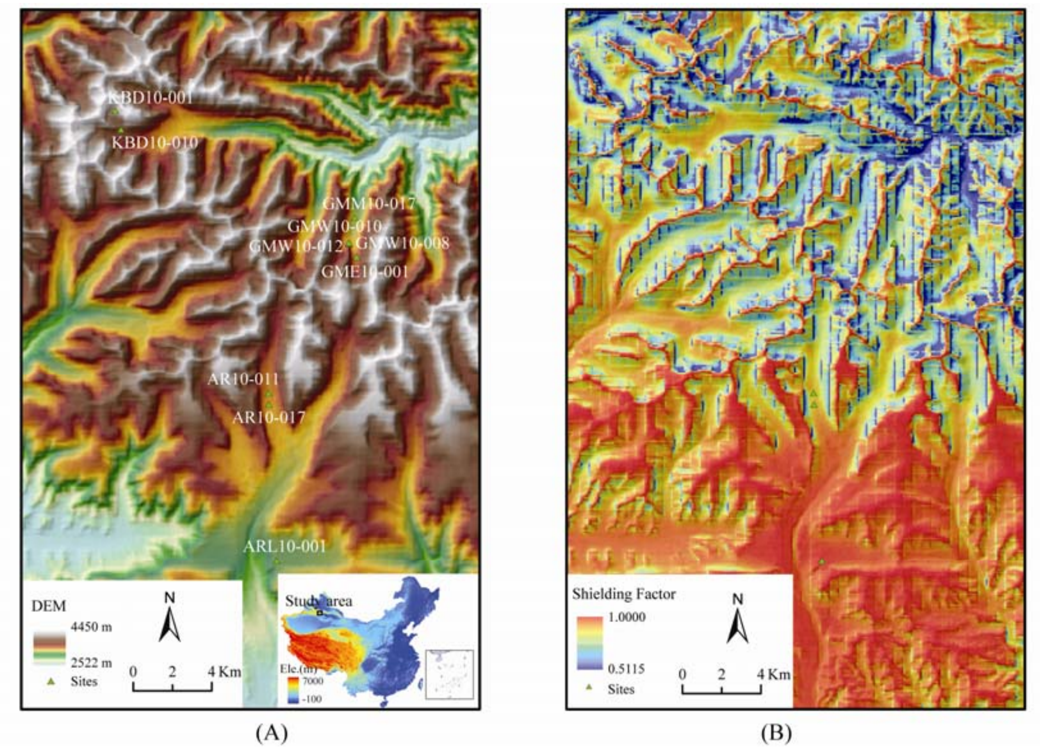

Figure 2 (A) The SRTM DEM of the study area in central Tian Shan and sites with the measured topographic shielding parameters. (B) DEM-derived topographic shielding factor for the whole area using 5° interval in azimuth and 2° interval in elevation angles. The strips appeared in the topographic shielding map indicate potential errors caused by the low quality of the SRTM DEM in this region.

Table 1 Field measured and model-derived topographic shielding factors (5° interval in the azimuth angle and 2° interval in the elevation angle) from central Tian Shan, China

Sample ID	Location	Field measured azimuth-elevation pairs	FMSF	MDSF	RD
KBD10-001	43.1279°N 86.8221°E 3,968 m	(49.8, 36.5) (106.3, 27.7) (134.0, 12.6) (143.0, 2.0) (151.0, 3.0) (155.0, 2.0) (164.0, 5.5) (179.0, 2.5) (189.0, 6.7) (197.0, 4.3) (249.0, 23.9) (315.0, 33.0) (351.0, 26.8)	0.9291	0.9388	0.97
KBD10-010	43.1192°N 86.8257°E 3,823 m	(95.4, 0.0) (109.3, 5.8) (134.0, 6.0) (143.0, 3.0) (167.0, 11.0) (192.0, 6.7) (211.0, 15.0) (225.0, 10.0) (243.0, 15.0) (266.0, 22.0) (300.0, 25.0) (333.0, 20.0) (345.0, 15.0)	0.9874	0.9792	0.82
GME10-001	43.0605°N 86.9734°E 3,535 m	(19.5, 3.3) (65.0, 28.0) (95.0, 34.0) (130.0, 25.0) (138.0, 28.0) (163.0, 13.5) (171.0, 16.7) (178.0, 13.5) (193.0, 19.0) (198.0, 18.5) (209.0, 19.0) (218.0, 24.5) (223.0, 22.0) (272.0, 28.0) (337.0, 9.6) (348.0, 3.4)	0.9567	0.9534	0.33
GMW10-008	43.0666°N 86.9688°E 3,509 m	(28.0, 2.5) (90.0, 25.0) (116.0, 24.0) (133.0, 18.0) (140.0, 25.0) (158.0, 15.0) (168.0, 25.0) (205.0, 15.0) (269.0, 30.0) (340.0, 15.0) (357.0, 3.3)	0.9677	0.9538	1.39
GMW10-010	43.0667°N 86.9687°E 3,500 m	(28.0, 2.4) (90.0, 25.0) (116.0, 24.0) (133.0, 16.7) (140.0, 19.5) (152.0, 15.7) (162.0, 17.7) (167.0, 24.0) (196.0, 12.0) (205.0, 10.0) (214.0, 12.8) (219.0, 11.8) (267.0, 29.8) (318.0, 23.0) (340.0, 14.6) (357.0, 3.5)	0.9708	0.9672	0.36
GMW10-012	43.0671°N 86.9684°E 3,486 m	(29.0, 2.6) (92.0, 25.0) (117.0, 24.0) (134.0, 17.0) (140.0, 19.7) (148.0, 15.8) (160.0, 16.0) (166.0, 23.0) (177.0, 15.0) (182.0, 17.5) (204.0, 10.0) (213.0, 13.0) (218.0, 12.0) (265.0, 31.0) (317.0, 24.0) (341.0, 15.5) (359.0, 3.7)	0.9690	0.9672	0.18
GMM10-017	43.0787°N 86.9722°E 3,363 m	(34.0, 4.3) (130.0, 25.0) (167.0, 8.8) (172.0, 9.7) (175.0, 8.7) (183.0, 13.0) (189.0, 12.0) (199.0, 10.0) (220.0, 25.0) (288.0, 35.0) (350.0, 4.4)	0.9641	0.9588	0.53
AR10-011	42.9978°N 86.9183°E 3,509 m	(0.7, 6.7) (10.3, 4.5) (14.1, 6.9) (15.0, 6.5) (30.0, 17.0) (77.0, 21.0) (127.0, 6.0) (130.0, 3.0) (169.0, 1.3) (173.0, 4.4) (285.0, 24.5) (320.0, 12.5) (326.0, 13.5) (350.0, 11.0) (357.0, 7.0)	0.9869	0.9780	0.89
AR10-017	42.9926°N 86.9184°E 3,487 m	(0.0, 10.7) (20.0, 8.2) (30.0, 15.0) (50.0, 12.5) (89.0, 27.0) (117.0, 20.0) (131.0, 21.0) (155.0, 13.0) (173.0, 0.0) (183.0, 1.2) (191.0, 3.4) (196.0, 3.0) (260.0, 33.0) (317.0, 20.0) (350.0, 17.0)	0.9688	0.9781	0.93
ARL10-001	42.9209°N 86.9235°E 3,281 m	(19.0, 8.4) (62.0, 5.5) (88.0, 2.3) (124.0, 4.5) (175.0, 3.0) (179.0, 3.7) (204.0, 4.2) (209.0, 2.8) (213.0, 4.1) (215.0, 3.3) (217.0, 4.0) (241.0, 2.0) (257.0, 2.7) (263.0, 0.6) (265.0, 0.8) (268.0, 0.0) (274.0, 0.9) (290.0, 0.7) (322.0, 4.5) (340.0, 3.4) (343.0, 4.7) (348.0, 4.1) (352.0, 5.7)	0.9997	0.9996	0.01

Note: FMSF= Field measured shielding factor; MDSF=Model derived shielding factor; RD= Relative difference (%)

interval in azimuth and a 2° in elevation angles (Figure 2B, Table 1). Results indicated that field-measured and model-derived topographic shielding factors are consistent with a strong positive regression ($y = 0.823x + 0.1691$, $R^2 = 0.8511$, Figure 3) and relative differences of <1.5%. This suggests that the algorithm to use GIS hillshade function to calculate the topographic shielding factor is valid and that DEM can be used to derive the topographic shielding factors for individual sites and an area if the shielding from local minor topographic features can be ignored.

The sensitivity of DEM-derived topographic shielding factors was also examined using a set of azimuth and elevation angle intervals (Table 2, Figure 4). Results indicated that the DEM-derived topographic shielding factor at a given site is more sensitive to the changes in the interval of the elevation angles (2° to 20°), whereas it is relatively stable with different interval values of the azimuth angles (2° to 15°). The topographic shielding factor generally decreases with the increase in the elevation interval. The differences between 2° and 5° intervals are relatively small (<1.2%), but

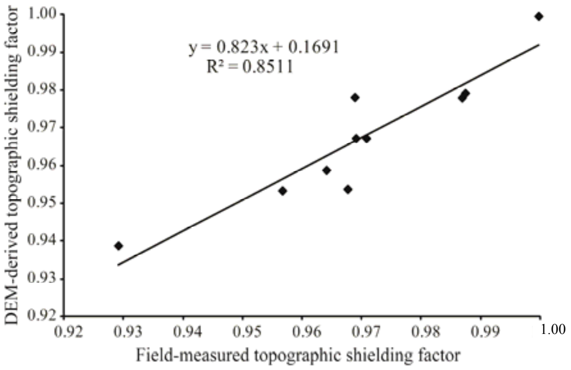

Figure 3 The regression relationship between field-measured and DEM-derived topographic shielding factors in central Tian Shan, China

increase with the increased intervals (>2.0% between 5° and 10° and even larger between 5° and 10° for some sites). The differences in the topographic shielding factor due to the differences in azimuth intervals are minor (<0.5% even between 2° and 15°). Therefore, using a relatively small elevation interval (<5°) and a moderate azimuth interval (5° to 10°) should be able to derive a realistic topographic shielding factor raster in a mountainous area.

4 Discussion

The python code and ArcGIS toolbox developed in this paper provide an easy and effective way to derive topographic shielding factors for an area and specific sample sites. The consistency between DEM-derived and field-measured factors in central Tian Shan validated the approach of using the GIS hillshade function to calculate the topographic shielding factor and indicated that DEM-derived factors can be used to replace field measurements if the shielding from local minor topographic features can be ignored. Therefore, this tool can save a significant amount of efforts in the field to interpret and measure topographic obstructions. Furthermore, the python code and ArcGIS toolbox can be integrated with other geoprocessing tools in ArcGIS Modelbuilder. Thus, it is possible to streamline and automate all cosmogenic nuclide related calculations in ArcGIS,

Table 2 DEM-derived topographic shielding factors using various intervals (2°, 5°, 10°, 15°) of azimuth and elevation angles

Sample ID	2, 2*	2, 5	2, 10	2, 15	5, 2	5, 5	5, 10	5, 15
KBD10-001	0.9392	0.9286	0.9087	0.8842	0.9388	0.9276	0.9065	0.8807
KBD10-010	0.9798	0.9739	0.9647	0.9445	0.9792	0.9737	0.9639	0.9433
GME10-001	0.9531	0.9456	0.9279	0.8916	0.9534	0.9470	0.9299	0.8933
GMW10-008	0.9544	0.9490	0.9362	0.9235	0.9538	0.9493	0.9360	0.9247
GMW10-010	0.9670	0.9626	0.9455	0.9270	0.9672	0.9620	0.9451	0.9247
GMW10-012	0.9670	0.9626	0.9455	0.9270	0.9672	0.9620	0.9451	0.9247
GMM10-017	0.9593	0.9500	0.9284	0.9085	0.9588	0.9502	0.9276	0.9081
AR10-011	0.9778	0.9713	0.9528	0.9390	0.9780	0.9714	0.9527	0.9397
AR10-017	0.9782	0.9719	0.9564	0.9420	0.9781	0.9725	0.9568	0.9435
ARL10-001	0.9995	0.9991	0.9969	0.9884	0.9996	0.9991	0.9969	0.9884
Sample ID	10, 2	10, 5	10, 10	10, 15	15, 2	15, 5	15, 10	15, 15
KBD10-001	0.9385	0.9292	0.9090	0.8837	0.9381	0.9278	0.9079	0.8832
KBD10-010	0.9795	0.9753	0.9666	0.9449	0.9796	0.9743	0.9673	0.9457
GME10-001	0.9542	0.9460	0.9289	0.8933	0.9538	0.9450	0.9293	0.8848
GMW10-008	0.9542	0.9498	0.9350	0.9260	0.9541	0.9506	0.9391	0.9247
GMW10-010	0.9672	0.9622	0.9451	0.9260	0.9664	0.9620	0.9451	0.9247
GMW10-012	0.9672	0.9622	0.9451	0.9260	0.9664	0.9620	0.9451	0.9247
GMM10-017	0.9588	0.9492	0.9272	0.9068	0.9586	0.9504	0.9237	0.9051
AR10-011	0.9779	0.9706	0.9513	0.9385	0.9783	0.9713	0.9544	0.9360
AR10-017	0.9787	0.9723	0.9560	0.9435	0.9781	0.9723	0.9596	0.9397
ARL10-001	0.9996	0.9991	0.9969	0.9884	0.9995	0.9991	0.9969	0.9884

Note: *The first number is the azimuth interval and the second is the elevation interval.

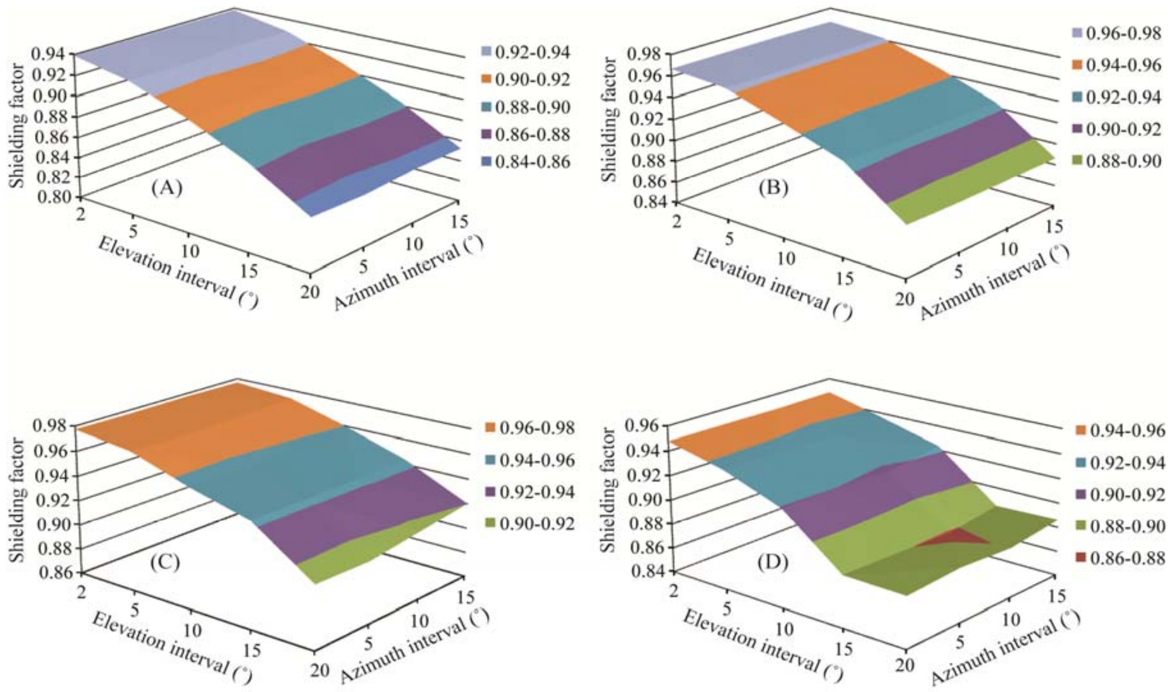

Figure 4 Variations in DEM-derived topographic shielding factors with different intervals of azimuth and elevation angles for sites: (A) KBD10-001; (B) GMW10-12; (C) AR10-011; (D) GME10-001

such as determining the production rates for a watershed and deriving the basin-wide spatially integrated erosion rate. Due to the global coverage of the STRM DEMs (except the polar regions), this tool has the potential to provide consistent results for different regions in the world to facilitate the comparison of cosmogenic nuclide results.

Even though the internally optimized hillshade function in GIS can speed up the calculation of the topographic shielding factor, deriving shielding factors for an area using small intervals of azimuth and elevation angles is still computational intensive and time-consuming. For example, it takes about one hour to calculate the topographic shielding factor in the study area of central Tian Shan using 5° intervals for both azimuth and elevation angles, but >28 hours when using 1° intervals. If the study area is bigger, it will be more time-consuming. However, the sensitivity analysis suggested relatively small differences for azimuth intervals. Therefore, using a relative small elevation interval (<5°) and a moderate azimuth interval (5° to 10°) should be able to derive a reasonable topographic shielding factor raster in a mountainous area. With the development of the computational techniques, parallelized algorithm and high performance computing using multi-cores have the potential to significantly improve the performance of the analysis and be able to calculate the topographic shielding factor for large study areas.

The quality of the DEM may affect the calculation of the topographic shielding factor. For example, the strips appeared in Figure 2B (the topographic shielding factor map for the study area derived using 5° interval in azimuth and 2° interval in elevation angles) indicate some potential issues in derived topographic shielding factor especially in high relief areas. Caution should be used for the derived values within the strips. Furthermore, the method discussed in this paper is only suitable to derive the topographic shielding factor for relative flat surfaces. In addition, it does not account for the potential shielding from local minor topographic features because these minor features cannot be represented in relatively coarse resolution DEMs (such as the SRTM DEMs). Therefore, caution should also be used when calculating the topographic shielding for deep slope surfaces and/or the sites with an obvious local topographic shielding.

5 Conclusion

This paper introduced a python code to calculate the topographic shielding factor for a given location or an area using DEM. This code can be imported into ArcGIS as a geoprocessing tool with a user-friendly GUI. The comparison between DEM-derived topographic shielding factors and field-measured values in central Tian Shan demonstrated the feasibility of this method and suggested that a small interval (<5°) in elevation and a moderate interval (5°-10°) in azimuth can be used to derive the topographic shielding factor for a mountainous area. This tool can save a significant amount of efforts in the field and has the potential to provide consistent results for different regions in the world to facilitate the comparison of cosmogenic nuclide results. However, the DEM-derived topographic shielding factor is potentially affected by the quality of the DEM and only suitable for relative flat surfaces. It also cannot account for the potential shielding from local minor topographic features. Therefore, caution should be used in applying this method in some situations.

Acknowledgements

This work was supported by the Professional Development Award of the University of Tennessee. The author thanks the editor and anonymous reviewers for their constructive suggestions.

References

Balco G (2011) Contributions and unrealized potential contributions of cosmogenic-nuclide exposure dating to glacier chronology, 1990-2010. Quaternary Science Reviews 30: 3-27, doi: 10.1016/j.quascirev.2010.11.003.

Balco G, Stone JO, Lifton NA, et al. (2008) A complete and easily accessible means of calculating surface exposure ages or erosion rates from ^{10}Be and ^{26}Al measurements. Quaternary Geochronology 3: 174-195, doi: 10.1016/j.quageo.2007.12.001.

Bierman P, Nichols KK (2004) Rock to sediment—slope to sea with ^{10}Be—rates of landscape change. Annual Review of Earth and Planetary Sciences 32: 215-255, doi: 10.1146/annurev.32.101802.120539.

Burrough PA, McDonell RA (1998) Principles of Geographic Information Systems. Oxford University Press, Oxford.

Codilean AT (2006) Calculation of the cosmogenic nuclide production topographic shielding scaling factor for large areas using DEMs. Earth Surface Processes and Landforms 31: 785-794, doi: 10.1002/esp.1336.

Desilets D, Zreda M (2003) Spatial and temporal distribution of secondary cosmic-ray nucleon intensities and applications to in situ cosmogenic dating. Earth and Planetary Science Letters 206: 21-42, doi: 10.1016/S0012-821X(02)01088-9.

Desilets D, Zreda M, Prabu T (2006) Extended scaling factors for in situ cosmogenic nuclides: New measurements at low latitude. Earth and Planetary Science Letters 246: 265-276, doi: 10.1016/j.epsl.2006.03.051.

Dunai TJ (2000) Scaling factors for production rates of in situ produced cosmogenic nuclides: a critical reevaluation. Earth and Planetary Science Letters 176: 157-169, doi: 10.1016/S0012-821X(99)00310-6.

Dunne J, Elmore D, Muzikar P (1999) Scaling factors for the rates of production of cosmogenic nuclides for geometric shielding and attenuation at depth on sloped surfaces. Geomorphology 27: 3-11, doi: 10.1016/S0169-555X(98)00086-5.

Gosse JC, Phillips FM (2001) Terrestrial cosmogenic nuclides: theory and applications. Quaternary Sciences Review 20: 1475-1560, doi: 10.1016/S0277-3791(00)00171-2.

Kong P, Fink D, Na CG (2009) Late Quaternary glaciation of the Tianshan, Central Asia, using cosmogenic ^{10}Be surface exposure dating. Quaternary Research 72: 229-233, doi: 10.1016/j.yqres.2009.06.002.

Li YK, Liu GN, Cui ZJ (2001) Glacial valley cross profile morphology, Tian Shan Mountains, China. Geomorphology 38: 153-166, doi: 10.1016/S0169-555X(00)00078-7.

Li YK, Liu GN, Kong P, et al. (2011) Cosmogenic nuclide constraints on glacial chronology in the source area of the Urumqi River, Tian Shan, China. Journal of Quaternary Science 26: 297-304, doi: 10.1002/jqs.1454.

Li YK, Harbor J (2009) Cosmogenic Nuclides and Geomorphology: Theory, Limitations, and Applications. In: Ferrari DM and Guiseppi AR (eds.), Geomorphology and Plate Tectonics. Nova Science Publishers, Inc., Hauppauge, NY. pp. 1-33.

Lifton N, Bieber J, Clem J, et al.(2005) Addressing solar modulation and long-term uncertainties in scaling secondary cosmic rays for in situ cosmogenic nuclide applications. Earth and Planetary Science Letters 239: 140-161, doi: 10.1016/j.epsl.2005.07.001.

Lal D (1991) Cosmic ray labeling of erosion surfaces: in situ nuclide production rates and erosion models. Earth and Planetary Science Letters 104: 424-439, doi: 10.1016/0012-821X(91)90220-C.

Nishiizumi K, Winterer EL, Kohl CP, et al. (1989) Cosmic ray production rates of ^{10}Be and ^{26}Al in quartz from glacially polished rocks. Journal of Geophysical Research 94(B12): 17907-17915, doi: 10.1029/JB094iB12p17907.

Stone JO (2000) Air pressure and cosmogenic isotope production. Journal of Geophysical Research 105(B10): 23753-23759, doi: 10.1029/2000JB900181.

Vermeesch P (2007) CosmoCalc: An Excel add-in for cosmogenic nuclide calculations. Geochemistry, Geophysics, Geosystems 8: Q08003, doi:10.1029/2006GC001530.

Wittmann H, von Blanckenburg F, Kruesmann T, et al. (2007) Relation between rock uplift and denudation from cosmogenic nuclides in river sediment in the Central Alps of Switzerland. Journal of Geophysical Research 112: F04010, doi: 10.1029/2006JF000729.

Zhao JD, Zhou SZ, He YQ, et al. (2006) ESR dating of glacial tills and glaciations in the Urumqi River headwaters, Tianshan Mountains, China. Quaternary International 144: 61-67, doi: 10.1016/j.quaint.2005.05.013.